Longitudinal Coupled-Bunch Oscillations in the Recycler Ring

Muhed Rana
Students in Science and Technology (SIST) Summer Internship Program at Fermi National Accelerator Laboratory
University of Maryland, Baltimore County
Baltimore, Maryland

Supervised by Dr. David Wildman
Fermi National Accelerator Laboratory
Batavia, Illinois

May 20th – August 9th, 2013

Abstract

In the NOνA project at Fermilab, the Recycler Ring will be used to create incredibly intense proton beams. The beams are found to interact with the Higher Order Modes (HOMs) of the radiofrequency (RF) cavities creating losses in the intensity of the beam, which is problematic due to the shift in focus to the intensity frontier. In this project, we measured the impedance of the HOMs of the cavity, measured the coupled bunch motion in the beam, and measured the effectiveness of the 157 (third harmonic) MHz dampers on the RF cavities. We have found that many of the losses in our cavity are the result of the fundamental and 9th harmonic modes and the other HOMs are heavily damped.

Introduction and Theory

Purpose

As a result of the completion of the LHC at CERN, the Tevatron, once the most energetic accelerator in the world, was shut down. The focus of Fermilab has shifted to creating intense beams of neutrinos to examine their currently unknown properties. A neutrino interacts very weakly with the environment; probabilistically only one in 10^{13} neutrinos react with the environment. The NOνA project consists of creating very intense proton beams in the Recycler Ring, injecting and accelerating them in the Main Injector. Afterwards, we will move the proton beams to the "Neutrinos in the Main Injector" (NuMI) beamline where they will collide with graphite blocks to create other particles such as pions. Pions eventually decay into neutrinos and will eventually diverge as they travel, analogous to a beam of light. To combat this issue, these pions will be focused in one direction by magnetic fields. These pions will eventually decay into muons and muon neutrinos in the same direction as the pions they decayed from. These neutrinos then reach the MINOS detector in Ash River, Minnesota. This paper describes the interactions between the proton beams and the HOMs inside a cavity of the Recycler Ring.

Bunches and the Recycler Ring

An accelerator operates by accelerating particles in "bunches" in synchrotronic motion. These bunches are large amounts (approximately 10^{13}) of particles traveling together in a packet with some characteristic phase; separate bunches are characterized by different phases. The bunches are kept stable by an RF waveform at an accelerating station. However, not all particles in a bunch have equal energies; some have higher energies and some have lower energies. An "ideal" particle in a bunch would be directly at the "zero-point" of a sinusoidal RF waveform during each rotation and would have exactly the energy necessary to remain stable and stay in the bunch. This ideal particle is known as the synchronous particle. The synchronous particle can be visualized in phase space as shown in Figure 1. A particle with slightly higher energy would arrive at the accelerating station sooner when the RF waveform has a negative value resulting in a loss of energy and will resultantly hit the RF pulse in a longer amount of time in its next accelerating cycle. Conversely, a particle with slightly lower energy would approach the waveform later when the pulse has a positive value resulting in a gain in energy and arrives sooner in its next cycle. Effectively, during each synchrotron period, each particle readjusts so as to approach the synchronous particle in energy and time differential, causing small oscillations in the bunch. Particles are considered stable when they are within a certain threshold; this is known as the separatrix and can be visualized as shown in Figure 1. [1]
[2]

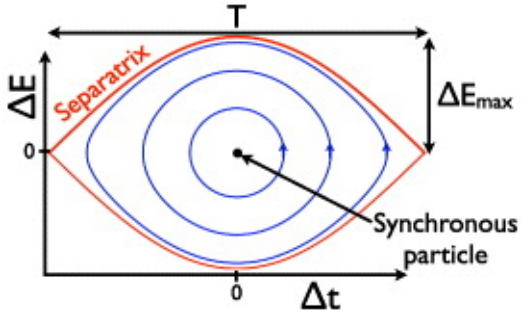

Figure 1; The separatrix of a bunch represented in phase space. A particle whose variations from the synchronous particles in energy and arrival time inside the separatrix is considered stable and remains inside the

bunch, contrary to a particle outside of the separatrix which will not be captured by the RF bucket. [3]

The bunches can be modeled as pulses represented by parabolas mapping current as a function of time. Each bunch is separated by times close to 18.9 ns (center-to-center), corresponding to a frequency of 52.809 MHz; they also have a base width of 8 ns. There are 82 bunches filled with protons followed by 2 bunches with zero particles in each batch deposited into the Recycler Ring, leading to a total of 6 batches in the ring at a time. There are 588 bunches allowed in the Recycler Ring, which means that 84 bunches in 7 batches can be filled with particles. However, this leads to problems; the magnetic field needs time to reach a maximum. This means that any bunches that exist in the region of increasing magnetic field (before it reaches a max) would leave the RF bucket and possibly damage the cavity. This issue is resolved by emptying two bunches in each batch. There are 6 batches at a time in the Recycler Ring as opposed to 7 because the 7th batch is used for injections from the Booster. The booster adds bunches to the Recycler Ring at a lower energy than those currently in the Recycler Ring. As time goes on, the injected particles are accelerated and eventually "stack" on top of the already existing bunches. This process is known as "slip-stacking."

The pulse function is normalized so that the total current in each parabola is $\frac{1}{588} \simeq .0017$ Amperes (so that 588 full bunches have a total current of 1 Amp). For our purposes, the entire batch consists of 82 full bunches and 506 empty bunches, representing 1 regular batch and 6 empty batches. The bunch is deposited into the Recycler Ring at a frequency of 52.809 MHz from the Booster. Due to the periodicity of the rotation, a fourier series can be taken allowing us to calculate the current flowing through the cavity. This also decomposes the function into a variety of HOMs; Figure 2 shows a plot of the fourier coefficients as a function of the harmonic number
(n).

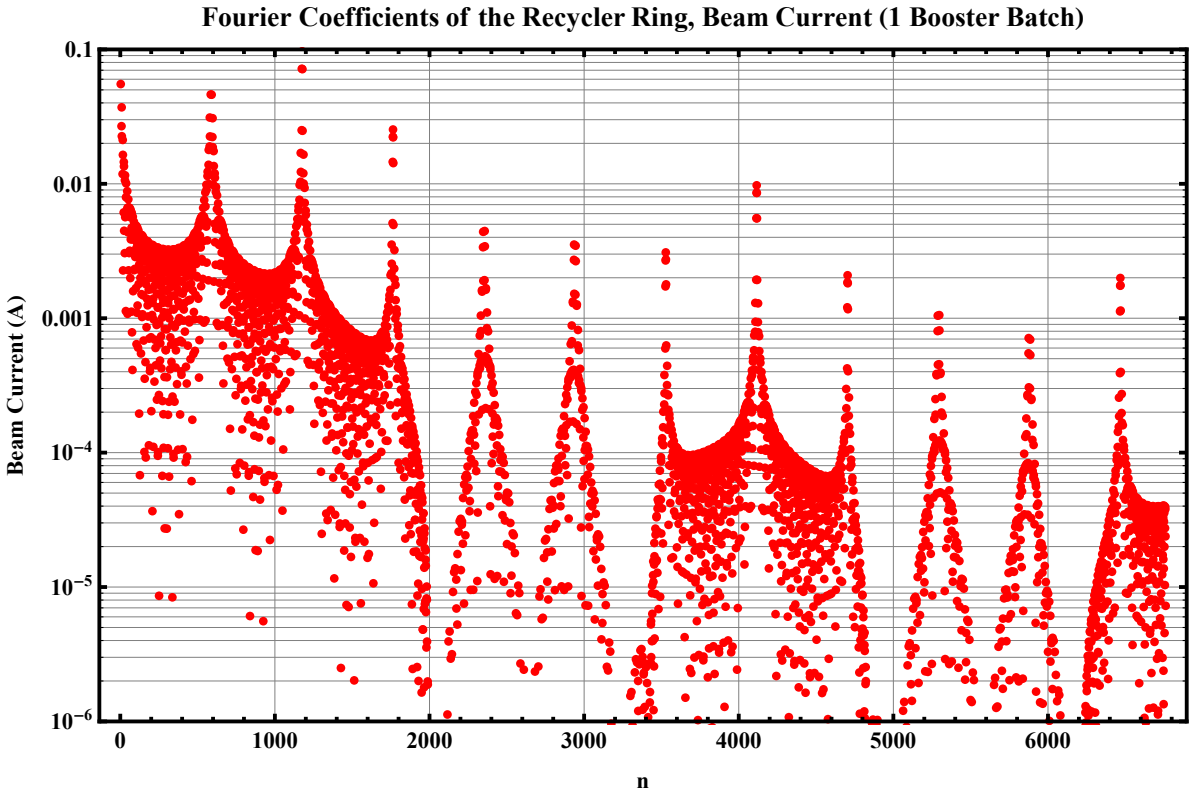

Figure 2; A plot of Fourier Coefficients as a function of the n in a log plot. The Fourier decomposition was taken using the frequency of the batch, $\frac{f_{RF}}{588}$, therefore n is an integer multiply of $\frac{f_{RF}}{588}$.

The Cavity

The Cavity is a quarter-wave resonator open on one end and shorted at the other. It operates at a fundamental frequency of 52.809 MHz. This means that only odd multiples of the fundamental frequency can resonate through this cavity. Figure 3 shows an illustration of the cavity.

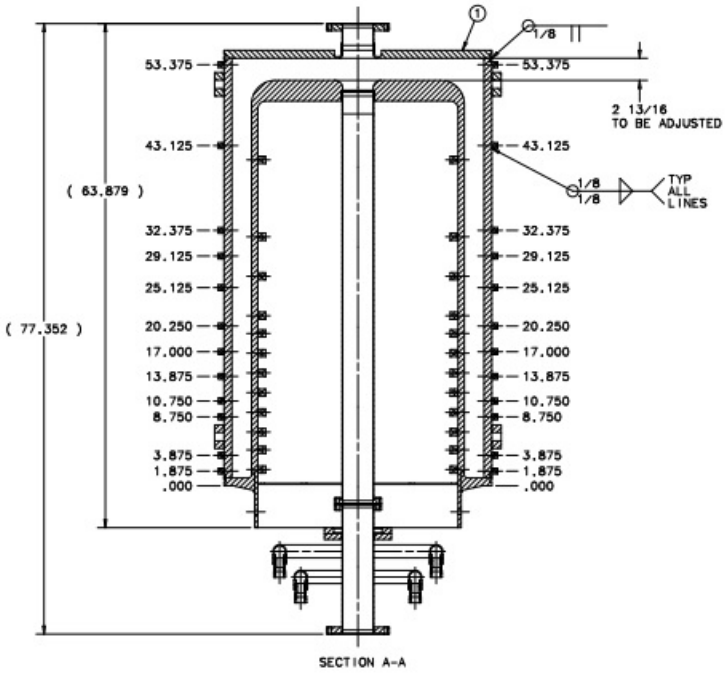

Figure 3; An illustration of the cavity. The length of the cavity is approximately 53", whereas the inner and outer radius of the cavity are 13.5" and 16" respectively. The boundary conditions require the top portion to be shorted out (0 V) whereas the bottom portion is at maximum voltage, resulting in solutions that are odd-integer multiples of a quarter wavelength.

The cavity has two primary sources of losses; the impedance of the shorted end and the impedance of the coaxial transmission line, which can be calculated using Equations 1 and 2.

$$R_{\text{line}} = x \sqrt{\frac{\mu_0 \pi f}{\sigma}} \ \frac{1}{2\pi}\left(\frac{1}{r_1}+\frac{1}{r_2}\right) \quad (1)$$

$$R_{\text{shorted end}} = \frac{1}{2\pi\delta\sigma}\,\text{Log}\left[\frac{r_2}{r_1}\right] \quad (2)$$

Where μ_0 is defined as the vacuum permeability, f is defined as the frequency of the fundamental mode, ℓ is the length of the center conductor, r_1 and r_2 are the inner and outer radii respectively, δ is the skin depth of copper, and σ is the conductivity of copper. The energy stored in the cavity resides entirely in the electromagnetic fields. This allows us to use the equation for the energy stored in an

inductor, assuming an ideal resonator with no gap capacitance. The energy stored in the cavity is shown by Equations 3 and 4.

$$L_{\text{gap}} = x\left(\frac{\mu_0}{2\pi}\,\text{Log}\left[\frac{r_2}{r_1}\right]\right) \quad (3)$$

$$E_{\text{stored}} = \frac{1}{\ell}\int_0^{\ell}\left(2 * \frac{1}{2}\,L_{\text{gap}}\,I^2\right)\text{dx} = \frac{1}{\ell}\int_0^{\ell}\left(L_{\text{gap}}\,I^2\right)\text{dx} = I^2\,\ell\left(\frac{1}{4} - \frac{1}{\pi^2}\right)\frac{\mu_0}{2\pi}\,\text{Log}\left[\frac{r_2}{r_1}\right] \quad (4)$$

We can then use this to find the quality factor Q of the cavity using Equations 5 and 6.

$$P_{\text{loss}} = \ell\int_0^{\ell}\left(I^2\,R_{\text{line}} + I^2\,R_{\text{shorted end}}\right)\text{dx} = I^2\,\ell\left(\frac{1}{4} - \frac{1}{\pi^2}\right)\sqrt{\frac{\mu_0\,\pi\,f}{\sigma}}\;\frac{1}{2\pi}\left(\frac{1}{r_1} + \frac{1}{r_2}\right) + I^2\,\frac{1}{2\,\pi\,\delta\,\sigma}\,\text{Log}\left[\frac{r_2}{r_1}\right] \quad (5)$$

$$Q = 2\,\pi\,f\,\frac{E_{\text{stored}}}{P_{\text{loss}}} \quad (6)$$

Combining equations 1 through 6 and simplifying we can derive an equation for Q for this cavity.

$$Q = \frac{2\sqrt{\pi\,\sigma\,\mu_0\,f}\;\ell\left(\frac{1}{4} - \frac{1}{\pi^2}\right)\text{Log}\left[\frac{r_2}{r_1}\right]}{\ell\left(\frac{1}{4} - \frac{1}{\pi^2}\right)\left(\frac{1}{r_1} + \frac{1}{r_2}\right) + \text{Log}\left[\frac{r_2}{r_1}\right]} \quad (7)$$

We can also find the shunt impedance of our particular cavity using Equations 8 and 9, using characteristic impedance of the coax line.

$$R_c = \frac{1}{2\pi}\sqrt{\frac{\mu_0}{\epsilon_0}}\;\text{Log}\left[\frac{r_2}{r_1}\right] \quad (8)$$

$$R_{\text{shunt}} = \frac{4}{\pi}\,R_c\,Q \quad (9)$$

Combining Equations 8 and 9 result in Equation 10 which calculates the theoretical shunt impedance of our cavity.

$$R_{\text{shunt}} = \frac{2\,\mu_0\sqrt{\frac{\sigma\,f}{\pi^3\,\epsilon_0}}\;\text{Log}\left[\frac{r_2}{r_1}\right]^2}{\left(\frac{1}{r_1} + \frac{1}{r_2}\right) + \frac{1}{\ell\left(\frac{1}{4} - \frac{1}{\pi^2}\right)}\,\text{Log}\left[\frac{r_2}{r_1}\right]} \quad (10)$$

Using Equations 7 and 10 with our cavity and the fundamental frequency f = 52.809 MHz, we calculate values of Q = 6000 and $R_{\text{sh}} = 77.8\,\text{k}\Omega$, and using the Fourier decomposition at n = 588 (f_{RF}) leads to V = 20.5 kV. The values of R_{shunt} for the HOMs can be approximated by the value of R_{shunt} at the fundamental divided by the square root of the Harmonic number. The value of R_{shunt} can be measured by Equation 11 below. [4]

$$R_{\text{shunt}} = \frac{V^2}{2\,P} \quad (11)$$

Harmonic Modes

There are two different classifications of modes present in the cavity; the Transverse Electromagnetic Modes (TEM) and the H_{m1} Ring Modes. The TEM modes are very simple to calculate and are odd multiplies of f_{RF}. The Ring modes are another type of mode that exist within the cavity. Note that there are a few other types of ring modes, H_{mn} and E_{mn} but these do not contribute to this particular type of cavity because their cut-off wavelengths are a function $r_2 - r_1$; both values are very close so calculating the frequency from these calculated wavelengths results in frequencies whose smallest value is in the GHz range. We are concerned with frequencies up to the 11th TEM mode, whose frequency is around 580 MHz. However, the cut-off wavelength of the H_{m1} mode is in a much more reasonable wavelength range. The value of the cut-off wavelength is shown in Equation 12.

$$\lambda_{cutoff} = \frac{\pi (r_1 + r_2)}{m} \quad (12)$$

m is defined as any positive integer. The wavelength of each Ring Mode is calculated by Equation 13.

$$\lambda = \frac{\lambda_g}{\sqrt{\left(1+\left[\frac{\lambda_g}{\lambda_{cutoff}}\right]^2\right)}} \quad (13)$$

Where λ_g is defined by Equation 14;

$$\lambda_g = \frac{4\ell}{n} \quad (13)$$

Where n is defined to be any odd positive integer. Ring modes vary in electric and magnetic field strength in both the radial and angular direction, and the distribution of the first three Ring Modes (H_{m1}, H_{m2}, and H_{m3}) are shown in Figure 4. [5]

Experimental Procedure

The measurements of R_{shunt}, the Voltage drop across the gap, and the quality factors were taken at the MI-60 building at Fermilab. An Agilent 8753ES S-Parameter Network Analyzer was connected to the cavity through a coaxial cable in the 1 and the 2 ports, which measures the loss in dB as a function of the frequency. Prior to making measurements, we had to calibrate the machine using a short, a 50 Ω resistor, and an open connector. We connected these into the 1-port in the network analyzer, one at a time, and used the calibration function to calibrate the machine to each of these elements. The Network Analyzer sends a signal through a coaxial cable connected to a magnetically coupled loop; the magnetically coupled loop's nominal input inpedance at 52.809 MHz is 50 Ω; the Network Analyzer sends a signal into the cavity and a certain amount is reflected back at certain frequencies. There is a capacitative pickup at the high voltage gap end of the cavity which measures approximately 1 V for every 89.5 kV at the shorted end. Figure 4 shows a sample measurement at approximately 156 MHz.

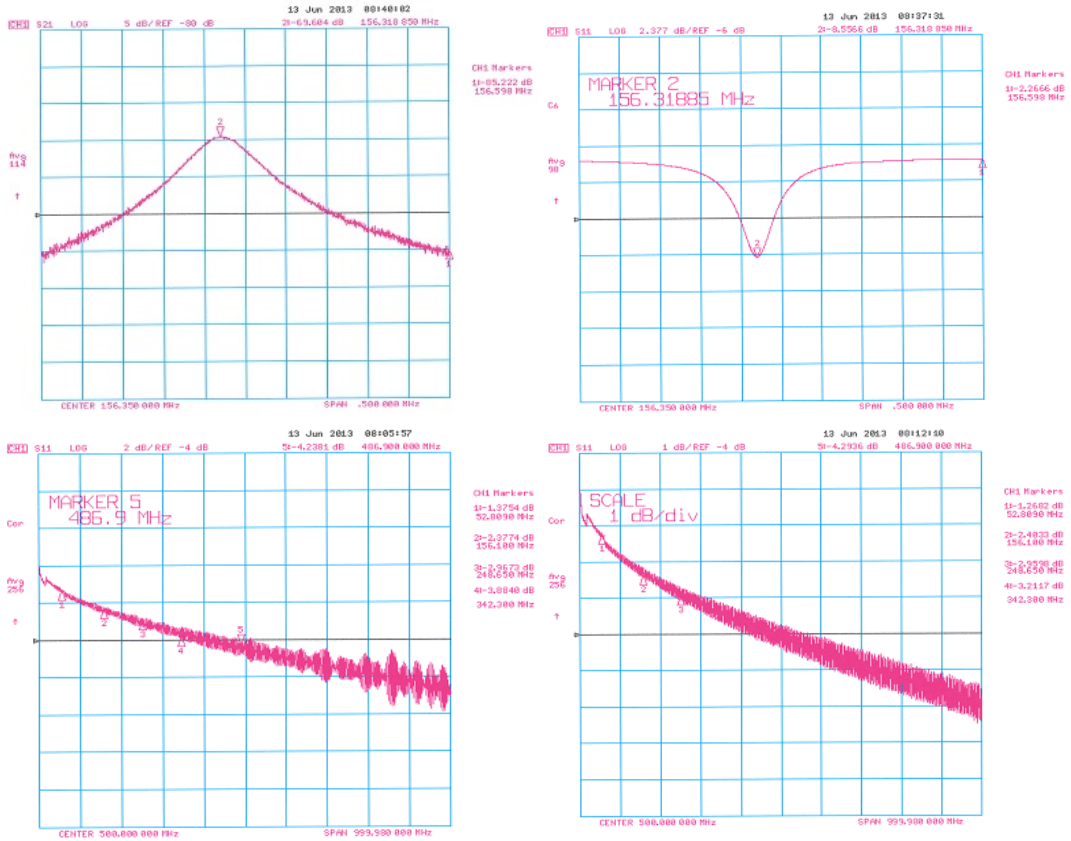

Figure 4; One set of measurements taken, associated with the third harmonic frequency. The top 2 measurements are zoomed into one frequency, wheraes the bottom two measurements are zoomed out to obtain more accurate values for the flat line voltage. The bottom left is for the power entering the drive and the bottom right is for the power through the gap monitor.

Both S11 charts on the right show the power inputted into the cavity. The flat line is the power entering the cavity, whereas the downwards peak is the power reflected by the cavity at that particular frequency. The values of power inputted and reflected are measured in dB, therefore the value of P_{loss} can be calculated by converting their logarithmic difference into Watts.

The primary purpose of S21 chart is to measure the voltage in the capacitative pickup. The voltage in the capacitative pickup can be measured by finding P_{loss} in the S21 chart. Due to the 50 Ω output resistor and the equation for Power (square of the voltage divided by the resistance), the value of the voltage drop in the capacitative pickup can be measured. However, as mentioned above, the capacitative pickup measures approximately 1 V for every 89.5 kV in the cavity at 52.809 MHz, and the effect changes for different frequencies.

A function was created to correlate the capacitative pickup to the frequency of the signal, modeling the capacitative pickup as a capacitor in series with a resistor, which are both in parallel with the another capacitor. Using this model, 1 volt is lost in the resistor/capacitor series combination whereas 89.5 kV are lost at the fundamental 52.809 MHz frequency in the lone capacitor. As the frequency increases the resistor/capacitor combination reports a lower voltage for every volt measured. The calculations and functions are shown in the Appendix; *Mathematica* Code: Calibrating HOM measurements. It should be noted that the capacitance is calculated using the physical attributes of the capacitor. It is

assumed that one of the capacitors is two concentric cylinders connected to a resistor. The lone capacitor also consists of two concentric cylinders but it is connected in parallel to the previous two elements. This allows us to measure the voltage drop associated with the S21 chart.

In order to take measurements of the harmonics, the measurement settings were set to start at around 5 MHz with a span of 10 MHz in the S21 setting. This displays many peaks and allows us to pinpoint each harmonic frequency. Starting from 5 MHz, if there were any peaks, they were zoomed in on (approximately a 500 kHz span) and a measurement of S21 and S11 were taken centered on that particular frequency with approximately 256 counts. This was repeated until we reached close to 600 MHz. The machine was set to measure the quality factor and the loss in dB. These measurements on the Network Analyzer were taken for two different gap monitors to identify modes, and by extracting the power from the loss in dB we can use Equation 11 to find R_{shunt}.

Modes were identified based upon their proximity to the calculated value as well as consistency in loss and phase between gap monitor signals (see Appendix, Table 1). Consistency between both values leads to the identification of an HOM. This allows us to find the harmonic frequencies even if they were to drift. One key factor is that the fundamental is always consistently close to 52.8 MHz and the 3rd Harmonic is sometimes damped, therefore it will always have a very low Q value. The fundamental Ring Mode is also known to be close to 141 MHz, and the consistency between both sets of measurements shows these factors. Often times, this results in measurements that diverse a large amount from their calculated frequencies, and that is acceptable because small fluctuations in wavelength will rapidly change the frequency.

The reason we look for similar losses and phases is because of the nature of TEM modes and the measurements. The measurements of the waves in the wall and gap cavities are physically 90 degrees apart; this means that if the waves measured at that particular frequency are TEM modes then the phase and loss would be the same because the electric and magnetic fields are perpendicular to one another an carry the same energy. However, for other types of modes, this could refer to any kind of wave; when the waves are not TEM modes they do not oscillate perpendicular to propagation and therefore it results in a wave that is not transverse. A way to visualize this is to imagine a large cylinder whose faces are perpendicular to the direction of propagation. This wave is propagating with a certain frequency that is not one of the harmonics, and it reaches both detectors at a different point in its propagation, leading to a difference in phase and loss if it is not a TEM mode.

To measure the current at each of the harmonic frequencies, beam was injected from the Booster into the Main Injector. The measurements were taken using an Agilent E4445A PSA Series Spectum Analyzer with -12 dB attenuation, with a 16 ns cable looking at the resistive wall monitor which has a resistance of 1 Ω. Figure 5 shows a sample measurement at the fundamental.

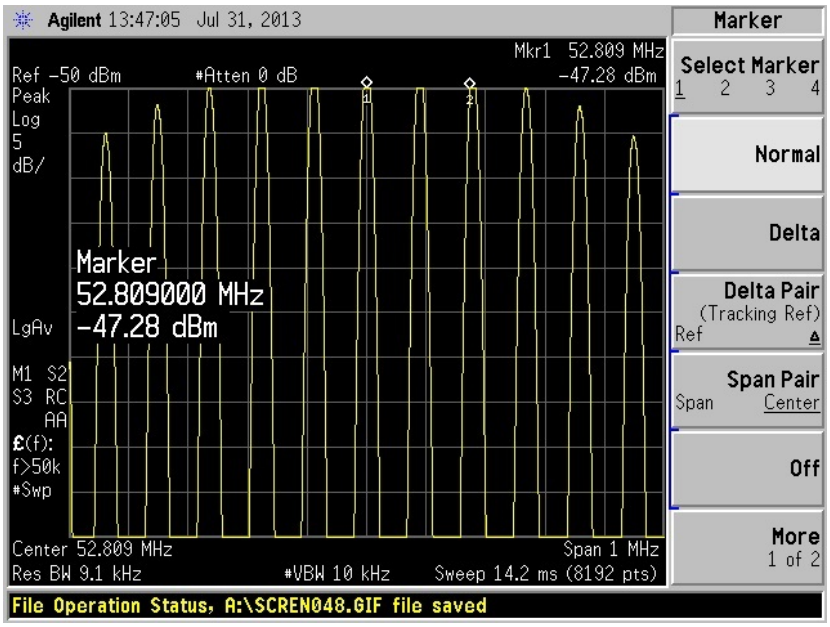

Figure 5; Measuring power loss in a spectrum analyzer. The actual power loss is the power loss measured above with 12 dB subtracted due to the RF splitters in the resistive wall monitor signal.

The power is calculated again through conversions from dBm to Watts. Following Equation 11, we can calculate the voltage based on the resistance in the coaxial connection. From here, we can calculate the current at each mode by dividing by 1 Ω, and the voltage loss at each of the harmonic frequencies can be calculated by multiplying each current at each frequency by R_{shunt}.

Experimental Results and Discussion

The experiments consisted of measuring R_{shunt} at each of the TEM Modes, the various modes existing inside the cavity, and the Beam Current using the Network Analyzer. The spectra were taken at many individual points analyzed at many different frequencies. These were measured using the S11 and S21 measurement options available on the network analyzer. Figure 4 above showed the measurements taken; these measurements can measure the value of R_{shunt} using Equation 14 below, with a sample calculation underneath.

This allowed us to calculate the value of R_{shunt} at each frequency; the Voltage and Power values can be found through taking the values at the marked points and converting their respective dB values to the proper SI units. Plugging into Equation 11 allows us to find the measured value of R_{shunt} The calculated values vs. the experimental values of R_{shunt} are listed in Table 1 below.

Frequency (MHz)	Theoretical (kΩ)	Experimental (kΩ)
52.809	77.8	75.8
156.098	45.0	20.4 (uda) / 2.45 (da)
248.496	34.9	5.8
335.843	29.5	22.5
428.645	26.0	21.3
570.736	23.5	2.6

Table 1; A comparison of measured values of R_{shunt} to the experimentally measured values resulting from Figure

4. “ud” refers to undamped and “da” refers to damped.

The value of R_{shunt} for the damped 3rd Harmonic was calculated by taking the ratio of the Q values due to Equation 9. The results are on the same order of magnitude undamped aside from the 5th Harmonic, and damped the experimental value of the 3rd Harmonic is very low indicating the dampers are effective in lowering the losses sustained by the 3rd Harmonic.

The modes were also measured through the network analyzer; Tables 2 and 3 respectively identify these modes as either TEM Modes or H_{m1} Ring Modes.

Frequency (MHz)	Q	Calculated Frequency (MHz)	Mode
52.809	5949.6	52.809	Fundamental
154.063	839.78	158.427	3rd Harmonic
247.595	9216.9	264.045	5th Harmonic
336.365	8905.1	369.663	7th Harmonic
475.141	16276	475.281	9th Harmonic
543.505792	14386	580.889	11th Harmonic

Table 2; identifying the Harmonic Frequencies in the cavity. The harmonics slightly contradict the values in Table 1 due to drift.

Frequency (MHz)	Q	Calculated Frequency (MHz)	Mode
141.293	4385.4	140.362	$m = 1, \frac{\lambda_g}{4}$
208.335	5383.7	218.089	$m = 1, \frac{3\lambda_g}{4}$
313.226	13416	310.193	$m = 2, \frac{3\lambda_g}{4}$
318.607	15811	321.379	$m = 1, \frac{5\lambda_g}{4}$
378.786	9037.2	386.592	$m = 3, \frac{\lambda_g}{4}$
389.109	17881	389.797	$m = 2, \frac{3\lambda_g}{4}$
419.858	4465.3	421.087	$m = 3, \frac{3\lambda_g}{4}$
428.798	16180	432.282	$m = 1, \frac{7\lambda_g}{4}$
480.541	9916.2	482.738	$m = 3, \frac{5\lambda_g}{4}$
486.652	15016	485.309	$m = 2, \frac{7\lambda_g}{4}$
496.523	9306.0	512.822	$m = 4, \frac{\lambda_g}{4}$
539.491	8305.9	539.302	$m = 4, \frac{3\lambda_g}{4}$
552.190	8477.4	546.179	$m = 1, \frac{9\lambda_g}{4}$
561.020	4944.3	562.689	$m = 3, \frac{7\lambda_g}{4}$

Table 3; identifying the Ring Mode Frequencies in the cavity.

There were many other modes measured using the Network Analyzer; these modes resulted from energy stored in the 9" coaxial line. These modes occur roughly every 14.3 MHz and the measurements of these modes are shown in Table 4. This 14.3 MHz value occurs due to the length of the coaxial cable (~1.75λ at 52.809 MHz) added to the gap between the inner and outer radius of the cavity (2.5"). This coaxial cable is connected to the power amplifier which is connected into the Network Analyzer to make measurements.

Frequency (MHz)	Loss (dB)	Mode Classification
14.3096	−68.674	TEM (1)
28.6667	−54.938	TEM (2)
42.9418	−42.504	TEM (3)
56.6482	−33.974	TEM (4)
72.3787	−48.049	TEM (5)
86.5932	−44.464	TEM (6)
100.827	−35.869	TEM (7)
114.755	−39.146	TEM (8)
128.718	−46.333	TEM (9)
141.751	−31.817	TEM (10)
151.616	−5.894	TEM (11)
181.245	−24.172	TEM (13)
194.540	−21.012	TEM (14)
208.682	−19.178	TEM (15)
221.500	−11.998	TEM (16)
235.005	−39.531	TEM (17)
266.590	−31.797	TEM (19)
280.275	−26.204	TEM (20)
310.000	−57.862	TEM (22)
323.185	−15.300	TEM (23)

Table 4; identifying the modes associated with the energy stored in the 9" coaxial line.

Finally, our results for the measurements for the current and voltage values found above are shown in Table 5 and compared to the Fourier Coefficients multiplied by the Shunt Impedances at those frequencies. In order to match up the values of current for each frequency, the theoretical and experimental values fundamental mode were normalized to 1 A. A measurement of the fundamental mode's current was found to be 5.4 mA and the calculated value was around .25 A. These were scaled to 1 A and measured values were multiplied by around 185 and the theoretical values were multipled by around 4.

Frequency (MHz)	V (theoretical, Volts)	V (measured, Volts)
52.809	75800	75800
154.063	1504.0	65.5641
247.595	899.43	35.7079
336.365	1720.2	110.582
475.141	1263.1	1372.08
543.505792	56.852	14.2224

Table 5; comparing theoretical voltage values to measured voltage values at each of the harmonic frequencies to see evidence of damping. The fundamental modes are expected to be the same. Note that the measured values for R_{shunt} were used to calculate each value.

It is easy to see that the measured values are in heavy disagreement with the theoretical values outside of the fundmental and 9^{th} harmonic modes. With reference to the 3^{rd}, 5^{th}, and 11^{th} harmonics, this is a result of damping that is already occuring at those modes as we can see from Table 1. Therefore, this means that only the 7^{th} harmonic displays inconsistency.

Conclusions and Further Study

From our data we can conclude that there is a small amount of voltage drop at every single harmonic frequency except the fundamental and the 9^{th} harmonic. This means that the dampers instilled onto those modes are doing their jobs and there aren't many losses due to the HOMs at those frequencies. We can also conclude that the shunt impedances are in reasonable (order of magnitude) agreement with the calculated values at all frequencies except for the 5^{th} and 11^{th} harmonics. The reasons for this are presently unknown (however the 11^{th} harmonic is expected to be weak) but this is also a sign of damping at those frequencies. Ultimately, this leads to the result that many of the beam losses in our cavity inside of the Recycler Ring occur at the fundamental and the 9^{th} harmonic modes.

To further our research on our cavity, it is necessary to investigate the damping of the 5^{th}, 7^{th}, and 11^{th} harmonic modes to reconcile the discrepancy between our calculated and measured values. It is also necessary to take measurements more often to account for the drift as well as identifying the HOMs with more consistency than we had originally (evident in the discrepancy in the frequency of the 11^{th} harmonic between Tables 1 and 2).

Acknowledgments (will add this later)

References

1. D.A. Edwards, M.J. Syphers, *An Introduction To The Physics Of High Energy Accelerators* (John Wiley & Sons Inc., New York, 1993). Vol. 1, p. 37
2. F.J. Sacherer, *A Longitudinal Stability Criterion For Bunched Beams*, CERN/MPS/BR, 73-1 (1973).
3. *The Decay of Ion Bunches in the Self-bunching Mode* - IOPscience. N.p., n.d. Web. 25 July 2013.
4. James E. Griffin, *A Numerical Example Of An RF Accelerating System* in *Physics of High Energy Particle Accelerators*, (Fermi National Accelerator Laboratory, Batavia, IL, 1982), p. 582
5. Elnaiem, Heba, *Prototype NOνA RF Cavity for the Fermilab Recycler Ring* (Fermi National Accelerator Laboratory, Batavia, IL, 2009) p. 10

Appendix

Table 1: Measurements made by the gap monitors (loss and phase are measured in dB and degrees, respectively)

Frequency (MHz)	Loss (Aisle)	ϕ (Aisle)	Loss (Wall)	ϕ (Wall)
52.92	-22.0	-129	-21	-133
103.2	-33.9	97	-44	108
117.2	-24.8	-123.3	-35	-151
131.5	-17.3	68.4	-34	170
144.503	-12.1	-90.8	-22.5	86
151.6	-8.5	-15.6	-8.9	169
159.1627	-5.21	-179.2	-3.6	-179.6
156.098	-44.7	101.6	-39.6	100.9
171.7	-11.0	141.9	-22	-68
213.66	-8.1	-137.82	-7.6	45
248.652	-1.7	-107.6	-.8	-109
301.21	-20	99	-9.5	-95
312.427	1.025	150.44	.14	-35
315.23	-2.3	80.8	-9.5	-92.5
322.12	-12	-31.8	-18	-22.3
328.587	-2.8	-81.7	-4.3	-86.7
342.34	-4.8	-65.1	-3.9	-69.6
360.95	-15.9	43.0	-16.8	43.0
373.65	-20.6	-51.9	-25	-57.1
386.82	-14.9	160	-22.5	151
389.27	-18	-40.4	-11	103.6
399.5	-16.5	79	-9.3	-91
416.22	-18	-28	-24	-31
429.1	-11.89	-115.0	-10.5	64.3
436.31	9.0	130.4	1.9	-54.9
443.6	-13.8	-174	-20.1	16
458.38	-12.0	99.36	-13	-98
470.38	-.52	62.8	-4.8	-115
474.65	-10	22.2	-12	-161
479.4	-7.2	141.4	-15.6	-53
486.86	-4.9	-22.1	-5.6	-21
496.04	10.54	-135.1	8.7	39.2
501.00	6.2	-50.6	3.1	121
512.618	3.4	-54	-2	-70
526.09	-26.7	-72.1	-6.3	-30.4
539.062	-1.41	-138.5	6.83	-148.5
543.422	-18.8	177.3	-13.4	-10.0
550.6	-8.51	77.7	-11.3	-128.6
555.20	-11.8	167.4	-10.2	-9.6
556.52	-9	-105.1	-14.2	44.1
564.3	-7.8	-122.2	-11.0	-123
574.68	-1.8	-11.6	4.0	-15.1

***Mathematica* Code**

Calculating Shunt Impedance:

```
r1 = 32 * .0254;
r2 = 27 * .0254;
ϵ = 8.85 * 10^-12;
μ = 4 π * 10^-7;
f = 52.8 * 10^6;
ω = 2 π f;
c = 2.9979 * 10^8;
β = ω / c;
gap = 3 * .0254;
A = (π * (r2/2)^2 + π (r1/2)^2 / 2 - π * (4 * .0254 / 2)^2);
Cgap = A / gap ϵ;
Z = Sqrt[μ/ϵ] / (2 π) Log[r1/r2];
ℓ = 50 * .0254;
Z Tan[β ℓ];
1 / (ω Cgap);
Cgap;
σ = 5.8 * 10^7;
ℓ = 53 * .0254 (1/4 - 1/π^2);
Q[f_] = 2 Sqrt[π μ σ f * 10^6] ℓ Log[r1/r2] / (ℓ (2/r1 + 2/r2) + Log[r1/r2]);
Shunt[f_] = 4/π Z Q[f];
```

Calibrating HOM measurements:

```
C2 = .02 / (99 999 * ωf)
Clear[ω, Z, i, V, Ztot];
Z[ω_] = Sqrt[(R1 / (1 + ω^2 C1^2 R1^2))^2 + (ω R1^2 C1 / (1 + ω^2 R1^2 C1^2) - 1 / (ω C2))^2];
i[ω_] = 100 000 / Z[ω];
Ztot[ω_] = Sqrt[(R1^2 + ω^2 R1^4 C1^2) / (1 + ω^2 R1^2 C1^2)^2];
V[ω_] = i[ω] Ztot[ω];
```

Fourier Series Coefficients:

```
Clear[α, t0, f]
t0 = 2.25 * 10^-9;
f = 52.809 * 10^6;
α = 1;
(*Plot[{1/588, -α((t - 1/f)^2 - t0^2)}, {t, 1/f - t0, 1/f + t0}, PlotRange→All]*)
a82filled0 =
  α f/588 Sum[Integrate[-((t - m/f)^2 - t0^2), {t, m/f - t0, m/f + t0}], {m, 0, 81}] // N;
α = 1/a82filled0 * 82/588;
a82filled0 =
  α f/588 Sum[Integrate[-((t - m/f)^2 - t0^2), {t, m/f - t0, m/f + t0}], {m, 0, 81}] // N;
a82filled[n_] = 2 f/588
   Sum[Integrate[-α ((t - m/f)^2 - t0^2) Cos[n 2 π f/588 t], {t, m/f - t0, m/f + t0}], {m, 0, 81}];
b82filled[n_] = 2 f/588 Sum[Integrate[-α ((t - m/f)^2 - t0^2) Sin[n 2 π f/588 t],
     {t, m/f - t0, m/f + t0}], {m, 0, 81}];
filled82list = {};
Do[AppendTo[filled82list, {i, a82filled[i]}], {i, 1, 588 * 11.5}]
ListLogPlot[filled82list,
 PlotStyle → {Red, PointSize[.008]}, PlotRange → {10^-6, .1}, PlotLabel →
  "Fourier Coefficients of the Recycler Ring, Beam Current (1 Booster Batch)",
 FrameLabel → {"n", "Beam Current (A)"}]
```